

The Dissolution of Fe in HCl from the Ilmenite Concentrate; Evaluating the Effect of Operating Parameters and Mutual Interactions



SEYED HOSEIN LAVASANI, EBRAHIM AZIMI, and MEHDI NASIRI SARVI

Selective HCl dissolution of ilmenite components for obtaining Ti or titanium dioxide (TiO_2) has been highly recognized due to its advantages, greater environmental friendliness, and simplicity, compared to H_2SO_4 and Cl_2 methods. The effect of numerous parameters has been studied with the one-factor-at-a-time method. The present study aimed to evaluate the effect of key operation parameters, such as acid-to-solid ratio (A/S: 5 to 20 mL/g), reaction temperature (T: 70 °C to 100 °C), and acid concentration (A pct: 15 to 30 wt pct), on the dissolution of Fe in HCl solution with the minimum Ti losses to the leachate from its abundant, domestic, and low-cost mineral source (Kahnnoj ilmenite concentrate) using central composite design–response surface methodology. After 90 minutes of leaching, the Ti/Fe (pct) in terms of dissolved amounts was selected as the process assessment response function. Based on the conducted experimental and statistical analysis, increasing the levels of parameters in the studied domain leads to an increase in Ti/Fe (pct), in the order of A pct > T > A/S. Two statistically significant mutual interactions between A/S-T and T-A pct, with 95 pct confidence level, were revealed for the first time in this study. The optimization strategy was set to the minimization of Ti/Fe (pct) by considering the objective of study and the selected response function. The A/S, T, and A pct were determined to be 5 mL/g, 70 °C, and 15 pct, respectively, for maximum impurity dissolution and minimum Ti loss to the leachate.

<https://doi.org/10.1007/s11663-019-01704-y>

© The Minerals, Metals & Materials Society and ASM International 2019

I. INTRODUCTION

THERE are over 20 minerals containing Ti, among which ilmenite (FeTiO_3), with about 89 pct, is the most frequent one.^[1,2] The Kahnnoj and Ghare Aghaj mines are considered the two biggest ilmenite deposits in Iran with over 150 and 56 million tons of proven Ti, respectively. Currently, efforts are in progress to obtain various Ti products from the produced ilmenite concentrate of the Kahnnoj mine. Although ilmenite is considered as a low-grade Ti source, it is regarded as the major source of Ti and relevant products.^[2] Titanium, especially titanium dioxide (TiO_2), has vast applications in different industries due to its unique properties, such as white pigment. In addition, it plays a significant role in different areas related to paper, ink, plastics, medicine, cosmetics and pharmaceuticals, ceramic, dye synthesis solar cells (DSSCs), catalysts, batteries, sensors, water purification, self-cleaning coats, stainless

steel coating, roofing granules, *etc.*^[2–9] Nowadays, nanomesoporous TiO_2 is largely used in DSSC industries due to its unique properties. Consequently, several studies have been conducted on the effect of operating parameters on the synthesis of these particles. Various synthesized compounds (*e.g.*, tertrabutyl orthotitanate,^[10,11] titanium isopropoxide,^[12–14] and titanium sulfate^[15]) are usually used as the source of Ti in the experiments (in laboratory), where natural Ti containing minerals, such as ilmenite^[16–18] and leucoxene,^[19] are considered as major sources for producing Ti in industry.

Two different procedures are currently employed in industry for treating Ti containing minerals, subjected to the mineral type.^[20] In the sulfate process,^[20–23] high concentrated sulfuric acid (80 to 95 pct) at 150 °C to 200 °C is used leading to the production of the TiO_2 pigment with anatase or rutile phase after reduction, clarification, hydrolysis, and calcination stages. Either ilmenite concentrate (45 to 65 pct TiO_2) or Ti-containing slag (79 to 86 pct TiO_2) can be used in this method.^[20] Further, different parameters influence the process efficiency and recovery such as particle size, acid concentration, temperature, reaction time, acid-to-solid ratio, and agitating rate.^[24–27]

SEYED HOSEIN LAVASANI, EBRAHIM AZIMI, and MEHDI NASIRI SARVI are with the Department of Mining Engineering, Isfahan University of Technology, Isfahan 84156-83111, Iran. Contact e-mail: eazimi@cc.iut.ac.ir

Manuscript submitted April 22, 2019.

Article published online October 11, 2019.

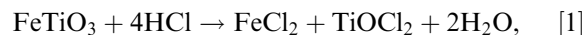
During the chloride process,^[28–30] the Ti is converted to the TiCl₄ gas in the presence of chlorine gas and petroleum coke at high temperatures (over 800 °C). Then, the purified TiCl₄ gas is oxidized to TiO₂ (pigment) by oxygen. Furthermore, it is possible to obtain the Ti in metal form when the purified TiCl₄ gas is reduced by Mg. Ilmenite is not industrially considered as a preferred resource for obtaining TiO₂ via the chlorine method due to the high Fe content of ilmenite, which results in consuming higher chlorine and forming iron chloride. Therefore, its Fe content should be reduced before reduction by chlorine gas in the case of using ilmenite. Several chlorine-based methods, such as Becher, Murso, Laporte, Austpac ERMS, Benelite, direct leaching, and smelting, can be addressed for synthetic rutile production. In all of these methods, the feed grade and process temperature are regarded as the most influential operating parameters.^[28,31]

Each method has its own advantages and disadvantages. However, feed grade, mineralogy, available technology, and facilities on the site, as well as environmental regulations, play a role in selecting the method. Unlike the sulfate process, which is a simple and noncontinuous technology, the chlorine method is regarded as a more recent and continuous process. The sulfate method is preferred to process ilmenite, range 40 to 86 pct TiO₂, with the products of either anatase or rutile phase depending on the calcination temperature, although with more environmental issues compared to the chlorine technology.^[20,32–35] A product with rutile phase is easier to obtain with the chlorine method, with lower operational costs, less waste material, and fewer pollution emissions.^[28,31] The chlorine method can be considered as two independent processes by using gaseous Cl in the leaching process or the HCl. The HCl leaching of iron from ilmenite avoids emission of gaseous sulfur oxides and ferrous sulfate by-products with minimum acidic water production.^[28] In this regard, there are several HCl regeneration methods for recycling the spent HCl.^[36] In addition, high acid consumption rates and process temperatures are considered as other disadvantages of the H₂SO₄ method compared to the HCl method.^[37]

Berkovich^[38] developed a room-temperature leaching procedure of the ilmenite by HCl. Further, he dissolved the Ti and Fe (over 80 pct) while other impurities remained in the solid phase. Next, the Ti was hydrolyzed and separated from the filtered solution as TiO₂. Imahashi and Takamatsu^[39] leached ilmenite directly with sulfuric acid, with low HCl concentrations (0.03 to 1.0 M). The results indicated that the increases in initial acid concentration and temperature are the most affecting parameters, which result in increasing the dissolution of Fe and Ti in HCl leaching. Some researchers evaluated the effect of particle size and ilmenite activation and reported that both can positively affect the Fe and Ti dissolution.^[3,40–42] Olanipekun^[40] focused on mixing intensity and found no significant effect on the Ti and Fe dissolution rate beyond a required minimum agitation rate. In another study, Olanipekun^[40] and Sasikumar *et al.*^[42] investigated the dissolution of Fe

and Ti in 2.3 to 11.5 M HCl in the temperature range of 50 °C to 100 °C. The results indicated that both acid concentration and an increase in the temperature during the leaching process can improve ilmenite dissolution. Further, Sasikumar *et al.*^[42] revealed that hydrolysis of Ti in the solution starts at temperatures over 70 °C in the acid-to-solid ratio of 10 mL/g and after 45 minutes leaching while using 8 M HCl. Similarly, Ti hydrolysis occurred at 100 °C and 12 M HCl in another study conducted by El-Hazek *et al.*^[3] focusing on the effect of pulp density in the range of 1/9 to 1/55 (solid-to-acid ratio). Based on the results, the pulp density could significantly affect the dissolution of Fe and Ti from ilmenite, which resulted in ilmenite losing its effect at high pulp densities. In other words, the dissolution rates of Fe and Ti become approximately equal. Furthermore, Vásquez and Molina^[43] indicated that the pretreatment of ilmenite by roasting leads to an increase in Fe dissolution kinetics and a decrease in the Ti dissolution rate. Further, an increase in the temperature negatively influenced the Ti and Fe dissolution within the range 700 °C to 1050 °C. In another study, Jabit and Senanayake^[44] studied the effects of HCl concentration, leaching time, and solid-to-liquid ratio on the thermally oxidized ilmenite at 900 °C and concluded that the dissolution of Ti decreases at higher acid concentrations and liquid-to-acid ratios. However, no significant decrease occurred in Ti dissolution after leaching for 4 hours.

Equation [1] presents the dissolution of ilmenite by HCl, and Eqs. [2] and [3] indicate the hydrolysis of the leached Ti (ions) to TiO₂.^[45,46]



As already mentioned, a large body of research emphasized the effect of various operating parameters on the dissolution of Fe, Ti, or other components of Ti containing minerals in order to obtain the purest Ti containing solid or selectively transfer Ti to the solution phase. All of the conducted studies used the one-factor-at-a-time method for evaluating the effect of different parameters on the designated process, without considering the possible mutual interactions between the parameters. The output can be different when there is an interaction, depending on the adjustment of two or more parameters rather than focusing on the individual parameter directly. In fact, the effect of one parameter on the response can be influenced by the value (level) of the other parameters. The existence of significant mutual interactions can contribute to better understanding of the parameters' influence on the output response and an improvement in process optimization in laboratory or industrial scale. Furthermore, dissimilar ranges were considered in different studies by focusing on a common parameter, and the order of optimizing parameters is usually different.

Therefore, the present study aimed to evaluate the possibility of obtaining the maximum amount of pure TiO₂ solid residual through leaching Kahnooj ilmenite concentrate with HCl solution. In fact, this study seeks to investigate the possibility of maximum Fe removal from ilmenite with minimum Ti loss to the leachate by HCl solution, determine the impact of the main influential operating parameters, and reveal any possible mutual interactions between them, as well as obtain the optimum levels of the studied parameters by considering their mutual interactions. The leaching time, leaching temperature, acid concentration, and pulp density were selected as the main operating parameters; their influence on the leaching phenomena was also statistically determined. In order to conduct the present study, the experiment design methods were employed to evaluate the effect of parameters on the Fe dissolution by HCl and to find significant mutual interactions of the parameters. In addition to the HCl dissolution of ilmenite components in a moderate temperature range, using the design of the experimental methods for simultaneous evaluation of the operating parameters' effect on the Fe dissolution, revealing the mutual interactions among the parameters, and taking advantage of statistical analyses and determining the significant interactions for optimizing the parameters for maximum Fe dissolution are highlighted as novel in the present study.

II. MATERIALS AND EQUIPMENT

In the present study, the ilmenite concentrate from Kahnooj (Kerman, Iran) was used. Dry/wet sieving was conducted for 15 minutes using a rotary sieve shaker and ASTM sieves of 38 to 500 μm , for determining the particle size distribution of the samples. In addition, major solid phases of the concentrate were determined by an X-ray diffraction (XRD) analyzer (AW-DX300, Asenware, China) at a 2θ range of 4 to 80 deg. Further, the chemical composition of the solid material was determined by an X-ray fluorescence spectrometer (S4PIONEER, Bruker, Germany). Accordingly, the amounts of Ti, Fe, and other elements in leach solution were determined by ICP-OES (Varian-735, Australia) with minimum detection limits of 0.05 and 0.1 ppm for Ti and Fe elements, respectively.

A 7.2 lit (12. \times 5-in.) wet Denver ball mill (60 rpm with 17- and 30-mm balls) with a ball-to-solid ratio of 10:1 was used for ilmenite concentrate grinding. The milling was conducted for 60 to 240 minutes, as needed, and the resultant pulp was dehydrated at 80 °C using a Memert oven. Then, a Universal 320R centrifuge (maximum 5000 rpm) with eight 50 cc tubes was used to separate the liquid and solid phases when conventional filtering of the samples was impossible after acidic leaching.

The high concentration lab grade HCl acid, 37 pct Merck, and distilled water (resistivity = 18.2 M Ω , pH 6.8, and density = 1 g/cm³) were used in leaching experiments or solid residuals washing (diluted HCl), if necessary.

A. Experimental Setup

In order to maintain a constant acid-to-solid ratio during the experiments, the necked flask was connected to a graham condenser linked to a LAUDA Alpha RA-12 circulator with accuracy of ± 0.5 °C and was adjusted to -8 °C outflow. Then, an IKA RH basic two magnet stirrer hot plate was used to mix and heat the solid-acid mixture to the predetermined temperature.

B. Ilmenite Concentrate Characterization

As previously mentioned, the ilmenite concentrate was supplied from the Kahnooj processing plant. The concentrate had a narrow size distribution due to the previous treatment necessities (such as crushing, grinding, and physical separation). Based on dry sieving, all particles were found to be finer than 500 meters. Further, 80 and 29 pct of the concentrate were determined to be finer than 425 and 210 μm , by weight.

Table I indicates the chemical composition of the ilmenite based on XRF analysis, where Fe and Ti oxides are considered as the major components. Based on the presented composition, the ilmenite concentrate has a maximum of 23.6 pct leachable Ti.

Figure 1 displays the XRD pattern for ilmenite concentrate. As shown, the major solid phase is ilmenite, followed by anorthite as the next main phase, although it is not dominant. Based on the Rietveld method,^[47] the weight fraction of the ilmenite phase was estimated to be about 94 pct (± 5 pct error) of the total solid.

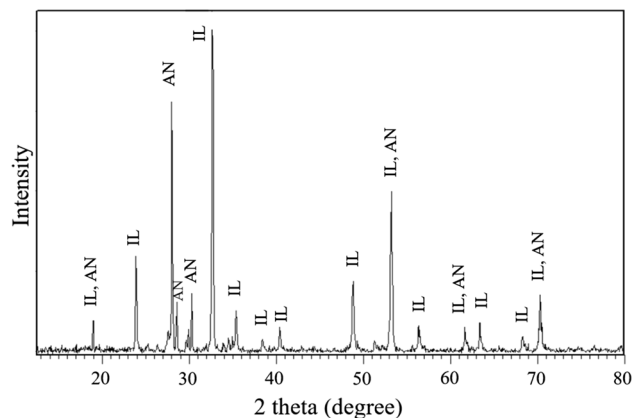


Fig. 1—XRD pattern of Kahnooj ilmenite concentrate (ILs: ilmenite and AN: anorthite).

Table I. Chemical Composition of Ilmenite Concentrate

Compound	Fe ₂ O ₃	TiO ₂	SiO ₂	CaO	Al ₂ O ₃	MgO	MnO	Na ₂ O	P ₂ O ₅	Other
Concentration (Wt Pct)	43.49	39.38	8.56	2.93	1.99	1.85	0.97	0.31	0.11	0.31

III. EXPERIMENTS

For each of the experiments, 20 g of dry ilmenite powder was added to the previously measured and heated HCl solution, which was diluted according to the decided condition. The reaction temperature was monitored with a thermometer (± 1 °C) and adjusted by the hotplate. After reaching the determined leaching time, the slurry was cooled immediately by ice, and then liquid and solid phases were separated through centrifuging for 7 minutes at 4000 rpm. Next, the collected solids were rinsed with dilute HCl and dried to obtain the solid dissolution ratio. The rinse acid was collected and added to the purified liquid in order to minimize Ti loss and analytical errors. The amount of dissolved Ti and Fe in HCl was determined *via* ICP-OES analysis of the collected leachate for any individual test.

A. Response Surface Methodology

In order to evaluate the effectiveness of the independent factors on the determined responses, different approaches have been selected by researchers, especially through the one-factor-at-a-time method.^[48,49] Due to the complexity of the phenomena, different results may be obtained from the effectiveness of the parameters, mostly depending on the level and parameter that were examined first. Therefore, implementing design-of-experiment methods can minimize the risks of possible mutual interactions between parameters since these methods take advantage of mathematical and statistical analysis to evaluate the effect of parameters on the responses. Statistical analysis provides proper context to reduce the number of necessary experiments, while the same objectives could be achieved without any loss in the accuracy of the results.^[50–52]

In order to reach the desired optimum response, the developed response surface could be used for optimizing the parameters and determining the levels of the factors. Practicing response surface methodology requires (1) collecting a reliable data set of parameters and responses, (2) establishing a proper mathematical model, and (3) identifying direct and mutual interactions of the parameters. The developed model could be used for predicting the optimum condition for the designated goal.^[51–53]

In the present study, the central composite design (CCD) was used since it provides a similar output as the three-level full factorial design, with a comparable confidence level, but with relatively less tests. Fitting second-order polynomials is another advantage of the CCD, where the mutual interactions of nonlinear parameters could be revealed along with their linear

interactions.^[50,51,53] The details of how any responses are modeled based on the input parameters, error determination, error minimization strategy, and regression coefficient determination for developing a representative response surface have been discussed thoroughly in different studies.^[51,54–56]

B. Design of Experiments and Evaluation Criteria

In the present study, the effects of reaction temperature, acid-to-solid ratio (pulp density, volume, and weight), acid concentration (weight percentage), and leaching time on the HCl leaching of ilmenite concentrate were evaluated. Based on the initial test results, the leaching time was set to 90 minutes and the influence of the three remaining parameters was studied using the CCD method. The actual and coded values of the parameters (factors) are presented in Table II. The levels of the parameters were selected based on the preliminary leaching experiments, as well as on the available literature.

Considering the objective of this study, the best HCl leaching result could be addressed as the minimum Ti dissolution from the concentrate while the maximum dissolution of Fe and other compounds is occurring. The Ti/Fe (pct) was selected as the response function in terms of the dissolved amounts of both elements for each experiment. In fact, this response can simultaneously consider both minimum dissolution of Ti and maximum dissolution of Fe to the leachate, if the lowest level of Ti/Fe (pct) is reached. The commercial DESIGN EXPERT*

* DESIGN EXPERT* is a trademark of State-Ease Inc., Minneapolis, MN.

software (trial version)^[57] was used to establish models and evaluate the effects of parameters and mutual interactions.

IV. RESULTS AND DISCUSSION

A. Ilmenite Preparation and Leaching Time Determination

As discussed, individual samples were prepared by wet grinding for 60, 90, 120, and 240 minutes, and a combination of wet and dry sieving was performed to determine their size distribution. Based on the sieving results, grinding more than 60 minutes had no significant effect on the fineness of the prepared powder.

Table II. Symbols, Actual, and Coded Levels of the Parameters Used in the CCD

Variable	Name	Units	Lower Level (– 1)	Central Level (0)	High Level (+ 1)
Acid-to-Solid Ratio	A/S	mL/g	5	12.5	20
Reaction Temperature	T	°C	70	85	100
Acid Concentration	A pct	wt pct	15	22.5	30

The prepared XRD patterns of the ground samples (not included) presented no phase change due to an increase in grinding time. Therefore, the 60-minute grinding time was determined for solid material preparation by considering the particle size distribution and the energy requirements in industrial levels, leading to the grinding ratio of 12.5 (F_{80}/P_{80}).

Four leaching tests were conducted to verify the effect of leaching time (60, 90, 120, and 240 minutes) on the dissolution of the prepared (60-minute milled) solid material. The acid-to-solid ratio of 10 (acid volume/solid weight) and 20 pct HCl solution were considered for leaching 20 g of ilmenite with the mixing speed of 350 rpm. The relative remaining solid weights for 60, 90, 120, and 240 minutes leaching times were 67.4, 67.1, 66.4, and 63.8 pct, respectively. Considering almost constant solid recoveries, the 90-minute leaching time was selected to continue with the main experiments.

B. CCD Experiments

The coded values of the parameters for the 19 designed CCD experiments along with Ti/Fe (pct) for each experiment are presented in Table III. The runs 6, 9, 12, 18, and 19, as the five duplicated tests, were conducted in a random order to estimate the level of error, check repeatability, and minimize the systematic errors effect by analyzing the collected data.

There would be some Ti losses to the leachate under any circumstances, which should be avoided for maximum recovery of Ti in the next step. The dissolved Ti and Fe amounts were obtained based on the ICP-OES analysis of the leachate solutions and conducted mass balance calculations for each run. Consequently, the Ti/Fe (pct) was calculated based on the experiment results.

Table III. CCD Experiment Conditions and Corresponding Response Functions

Run Number	Surface Levels			Ti/Fe (Pct)
	A/S	T	A Pct	
1	+ 1	+ 1	- 1	60.91
2	- 1	0	0	68.48
3	0	+ 1	0	89.74
4	+ 1	0	0	90.22
5	0	- 1	0	59.63
6	0	0	0	81.85
7	+ 1	- 1	+ 1	90.26
8	- 1	+ 1	+ 1	82.60
9	0	0	0	80.20
10	+ 1	+ 1	+ 1	96.65
11	0	0	- 1	36.13
12	0	0	0	67.68
13	0	0	+ 1	95.60
14	- 1	- 1	- 1	17.02
15	- 1	- 1	+ 1	85.44
16	- 1	+ 1	- 1	28.92
17	+ 1	- 1	- 1	23.39
18	0	0	0	81.25
19	0	0	0	83.83

The analysis of variance (ANOVA) test was conducted to evaluate the significance of the effect of operating parameters and their mutual interactions on the response. An interaction occurs when the effect of one factor on the response depends on the level of other factors. The optimization of operating parameters based on the obtained response model was carried out next. Like most engineering aspects, the 95 pct significance level (p -values less than 0.05) was considered as the satisfaction criterion for the effectiveness of the parameters.

The excellence degree of the fitted model was evaluated based on several statistical parameters and criteria such as R^2 , adjusted R^2 (Adj. R^2), lack of fit, and coefficient of variation (C.V. pct). The determination coefficient (R^2) indicates the difference between the model prediction and lab test results. The Adj. R^2 presents any improvement in the model predictability when a new data point is added to the current model. The lack of fit determines the fitting quality of the data points to the model, which, for a properly determined model, should not be significant. The C.V. pct measures the scattering degree of the data by comparing the standard deviation with the mean. A lower C.V. pct is interpreted as a sign of better data reproducibility.^[53,58] The ANOVA test result and statistical details are represented in Table IV.

C. Effect of Parameters on Ti/Fe (Pct)

The statistically significant factors and mutual interactions (Table IV) affecting the Ti/Fe (pct) are given in Eq. [4]. Normalized values of the parameters were used to develop this polynomial response function. All three studied parameters affect Ti/Fe (pct) as well as two significant interactions between A/S-T and T-A pct. The effectiveness of the parameters can be considered in the order of A pct > T > A/S.

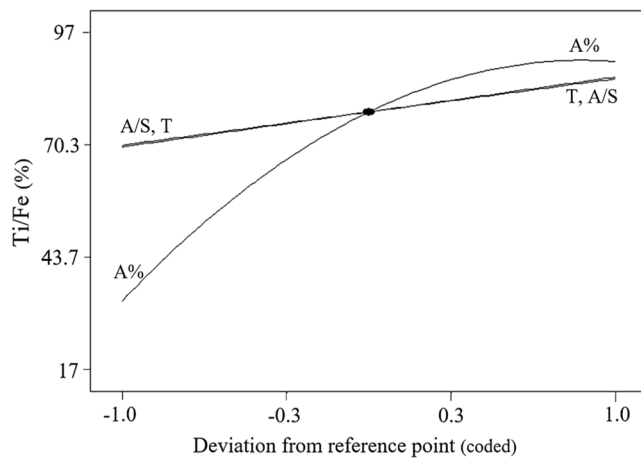
$$\begin{aligned} \frac{\text{Ti}}{\text{Fe}}(\text{pct}) = & 7.9 \times (\text{A/S}) + 8.31 \times (\text{T}) + 28.42 \times (\text{A pct}) \\ & + 4.36 \times (\text{A/S}) \times (\text{T}) - 5.73 \times (\text{T}) \times (\text{A pct}) \\ & - 16.41(\text{A pct})^2 + 78.1 \end{aligned} \quad [4]$$

Table IV. ANOVA Test Results for the Ti/Fe (Percent)

Source	Ti/Fe (Pct)		
	Mean Square	F-Value	p-Value Prob. > F
Model	1589.52	42.28	< 0.0001
A/S	623.78	16.59	0.0018
T	690.36	18.36	0.0013
A Pct	8075.25	214.78	< 0.0001
A/S-T	151.82	4.04	0.0697
T-A Pct	262.97	6.99	0.0228
(A Pct) ²	1275.04	33.91	0.0001
Lack of Fit	35.37	0.85	0.6009
R^2		0.9642	
Adj. R^2		0.9414	
C.V. Pct		8.83	

The significance of the presented model could be concluded based on the very low fisher's F test value (*i.e.*, p -value < 0.0001). Also, the p -value of 06009 proves its lack of fit. The R^2 , Adj. R^2 , and C.V. pct of this model are 0.9642, 0.9414, and 8.83 pct, respectively; therefore, the presented polynomial response function can statistically be used for response predictions at the experimental range of the parameters. As shown, the p -values of all three studied parameters are less than 0.05, meaning they will affect the response function with over 95 pct confidence level. The p -values of the T-A pct interaction are less than A/S-T and almost in the range of p -values of the individual parameters, showing the importance of these interactions on the dissolution operation and on the Ti/Fe (pct).

The perturbation and actual vs model prediction graphs are presented in Figures 2(a) and (b). In a perturbation graph, variations of each parameter are independently presented in its examined range, where its gradient indicates the effectiveness of that factor on the response function. The midpoint (arbitrary) of all variables is used in Figure 2(a). The x -axis of the plot shows the deviations from the reference point for each parameter. The existence of any curvature or steep slope indicates response sensitivity to the variations of that parameter.^[57] As shown, A/S and T have almost the same effectiveness on the response function when A pct and either A/S or T are set to their middle level. The A pct presents an increasing and nonlinear behavior. Such curvature can be interpreted either as a nonlinear behavior of A pct in the middle or upper range of its defined space or reaching its maximum effectiveness on the Ti/Fe (pct) somewhere before its maximum value (level + 1). In both cases, increasing A pct in its tested domain has a positive influence on the selected response (similar to A/S and T). The variations of either of A/S or T from their lower (-1) to higher level ($+1$) increases Ti/Fe (pct) from 69.11 to 85.4 pct, while an increase in A pct from its lower to higher level improves the response function over 56.32 pct.



Some studies emphasized the increasing effect of A/S, T, or A pct on the dissolution of Fe or Ti from ilmenite,^[38-42,46] while some reported a contrary effect. In some studies, an increase of A/S, T, or A pct reduced the total Ti dissolution.^[42,59] Such a decreasing trend is interpreted as the hydrolysis of the dissolved Ti in the solution and, consequently, precipitation on the solid material and falsely presenting a lower dissolution of Ti to the leachate from ilmenite.^[42,59-61] Such hydrolysis can be affected by the sources and alteration degree of the ilmenite, total TiO₂ content of the solid material, critical concentration of Ti ion, availability of the TiO₂ seeds in the leachate solution, and the elapsed process time.^[42,61] To the best of our knowledge, no study has been conducted on the possible interactions of the operating parameters and the effect of such interactions on the output of the ilmenite leaching process. As shown in Eq. [4], there are two statistically significant interactions.

1. Mutual interaction between A/S and T on the Ti/Fe (pct)

As shown in Table IV and Eq. [4], there are two significant mutual interactions of A/S-T and T-A pct at an almost 95 pct confidence level. The interaction between A/S and T is further illustrated in Figures 3(a) and (b) in the forms of two-dimensional (2-D) and contour plots. In order to present this interaction better, the level of A pct was set to 30 pct.

The existence of nonparallel lines, with or without an intersecting point in a 2-D interaction plot, is an indication of an interaction between two parameters (Figure 3(a)). Based on the results, 19.64 pct improvement occurs in Ti/Fe (pct) by increasing A/S from 5 to 20 mL/g, when T is set to 100 °C. However, A/S has no significant effect on this response, when T is selected to be 70 °C.

The contour plot of A/S-T interaction is presented in Figure 3(b). The Ti/Fe (pct) values for different sets of A/S and T can be extracted here. As shown by contour lines, the Ti/Fe (pct) is maximum when all three parameters are set to their highest level, but the Ti/Fe

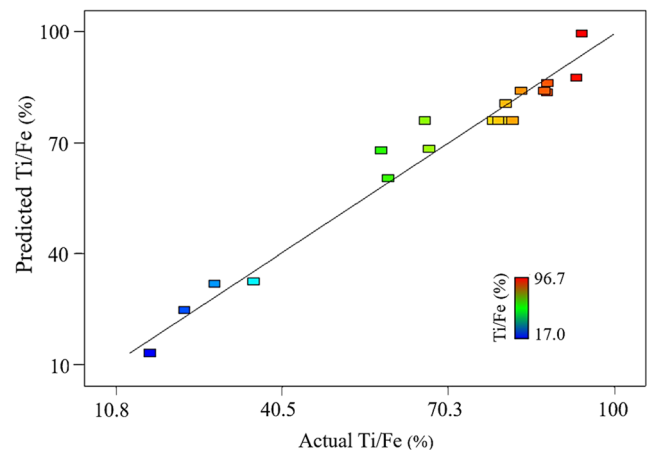


Fig. 2—(a) Perturbation plot and (b) actual vs model predictions.

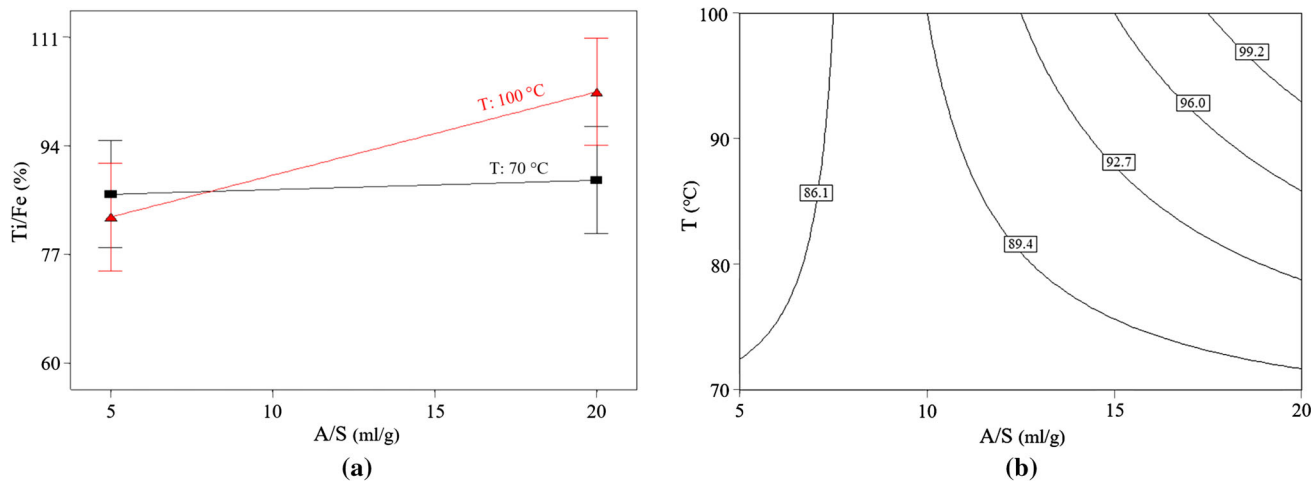


Fig. 3—Mutual interaction of A/S and T at A pct = 30 pct: (a) 2-D plot and (b) contour plot.

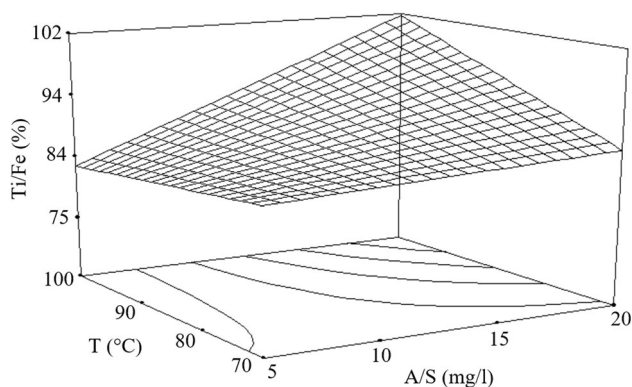


Fig. 4—3-D interaction plot of A/S and T at A pct = 30 pct.

(pct) drops over 15 pct by decreasing A/S and T to their lower levels (− 1). As the density of the contour lines indicates, these two factors (A/S and T) are more influential at their higher levels than their lower levels. As shown in Figure 3(b), once A pct is set to its higher level, the response is more sensitive for any step size change of A/S at higher levels of T rather than lower levels of it. The Ti/Fe (pct) increases about 14 pct once A/S increases from 5 to 20 mL/g at T = A pct = + 1. Due to the nature of the existing mutual interaction, the Ti/Fe (pct) is sensitive on any step size change of T at higher levels of A/S and A pct. A three-dimensional (3-D) surface plot of this interaction is illustrated in Figure 4.

In addition, Figure 4 reveals the curvature of the surface and the intense rise of this response once A/S and T are moving toward their higher level. The Ti/Fe (pct) decreases to 82 pct when A/S and T are reduced to − 1 and A pct is increased to + 1.

2. Mutual interaction between T and A pct on the Ti/Fe (pct)

Based on the results, a 97 pct significant interaction was observed between T and A pct. A 2-D and a contour plot of this interaction are illustrated in

Figures 5(a) and (b). In both plots, the A/S is set to its lowest level (5 mL/g). Figures 5(a) and (b) illustrate a typical representation of an interaction, where the effect of T on the response alters by variation of A pct at any certain level of A/S. For most of A pct, the higher Ti/Fe (pct) is achievable when higher levels of T are used, but once A pct reaches near its highest level, the existing interaction reverses the effect of T on the response. Finally, the maximum Ti/Fe (pct) occurs at T = 70 °C, A pct = 30 pct, and A/S = 5 mL/g.

As illustrated in Figure 5(b), any step size change of A pct has more of an effect on the response than T. Considering A/S at 5 mL/g, the Ti/Fe (pct) increases from ~ 25 to 75 pct by increasing A pct from − 1 to + 1 (15 to 30 pct) at almost the full range of T, while an increase in T from its lower level to its higher level has a minor increasing effect on the response at any level of A pct. In fact, based on the results in Figure 5(b), this response is somehow independent of T at higher levels of A pct as well as at A/S = 5 mL/g.

Figure 6 shows a 3-D surface plot of the interaction of T and A pct at A/S = 5 mL/g. The modeled surface indicates that the maximum response value can be obtained at higher A pct at almost any T and moves toward its minimum at A/S, T, and A pct of − 1, in such a conical surface mode. The variation of the Ti/Fe (pct) in the studied domain is over 80 pct.

V. OPTIMIZATION OF OPERATING PARAMETERS

Based on the objective of the study, Ti/Fe (pct) should be minimized through the variation of the operating parameters in order to eliminate Fe and other impurities through HCl leaching of ilmenite concentrate while sustaining maximum Ti in the solid phase. The optimization was conducted by using the results of the statistical analysis (Table IV) and the obtained response surface function (Eq. [4]).

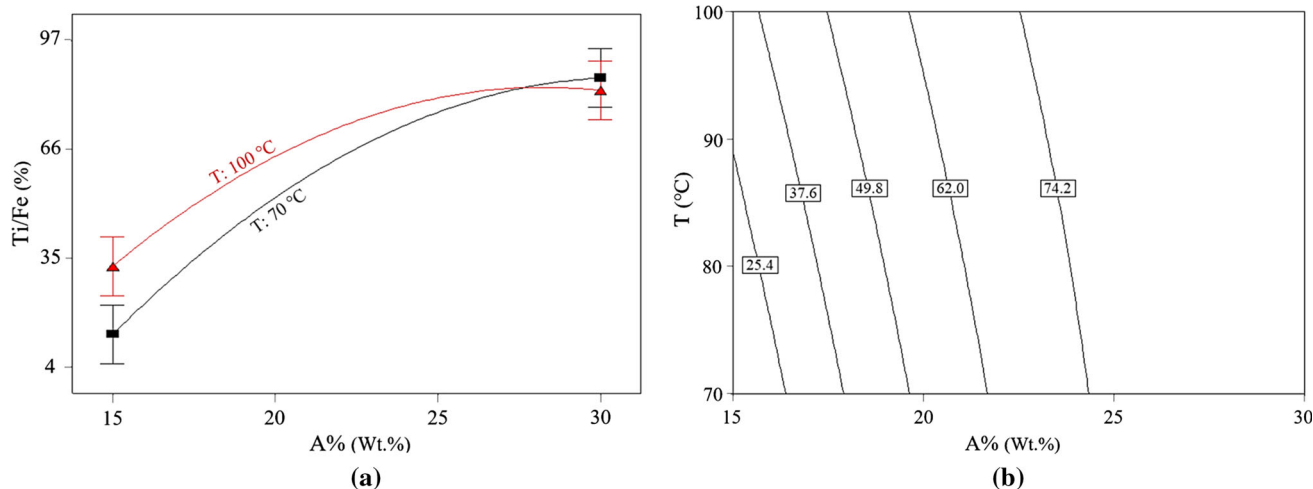


Fig. 5—Mutual interaction of T and A pct at A/S = 5 mL/g: (a) 2-D plot and (b) contour plot.

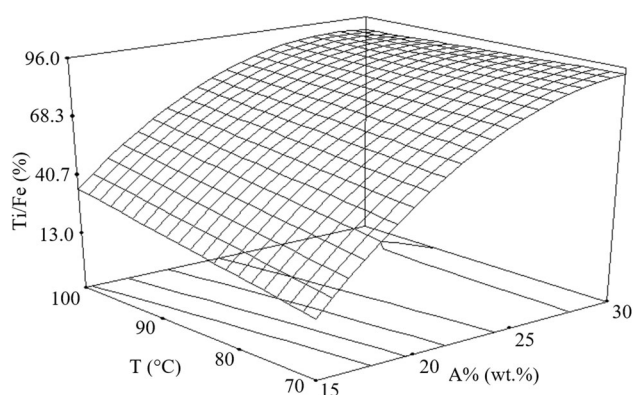


Fig. 6—3-D interaction plot of T and A pct at A/S = 5 mL/g.

The optimum levels of the operating parameters were determined to be A/S, T, and A pct in 5 mL/g, 70 °C, and 15 wt pct, respectively. As shown in Table III, these values are identical to run number 14.

A repeating test was conducted under 5 mL/g, 70 °C, and 15 wt pct in order to re-evaluate the model predictability and repeatability for the optimum condition. Then, the leachates were analyzed, and the dissolved Fe (pct), dissolved Ti (pct), and Ti/Fe (pct) were 10.81, 1.95, and 18.07 pct, respectively. Compared to the results of run 14, the relative difference of the tests in terms of the Ti/Fe (pct) was less than 5.8 pct.

Table V and Figure 7 present the chemical composition and XRD pattern of the solid residual for the optimization test, respectively. Considering the ilmenite concentrate chemical composition (Table I), an increase in TiO₂ and decrease in Fe₂O₃ could contribute to the selective dissolution of the components.

Regarding the comparison of the ilmenite concentrate and residual XRD pattern, the ilmenite phase is considered as the major phase for the solid residual, where some anorthite peaks are eliminated. Further, some rutile phase is raceable (individual or combined with ilmenite peaks), which results in widening the ilmenite peaks. The hydrolysis of TiO₂ develops the rutile phase in the solid residual.^[59,60]

VI. CONCLUSIONS

Based on the results, the selection of the Ti/Fe (pct) as the response function can successfully represent both minimum Ti loss to the leachate and maximum Fe removal from the solid phase. The 90-minute leaching time and wet grinding for 60 minutes were found as appropriate. The ANOVA test was used to evaluate the main parameters and their interactive effects on the response function. The effectiveness of the main parameters was determined in the order of A pct > T > A/S. Based on the validated response surface function, an increase in the intensity of the operating parameters increased the Ti/Fe (pct). Finally, two significant mutual interactions between A/S-T and T-A pct were discussed.

The operating parameters were optimized based on the Ti/Fe (pct) minimization concept, and the A, A/S, and T of 15 pct, 5 mL/g, and 70 °C, respectively, were determined as the favorable levels of the parameters for minimum Ti/Fe (pct) results. Finally, 5.8 pct deviations were reported by repeating the test results under the determined condition.

Table V. Chemical Composition of the Solid Residual (Optimization Test)

Compound	Fe ₂ O ₃	TiO ₂	SiO ₂	CaO	Al ₂ O ₃	MgO	MnO	Na ₂ O	Other
Concentration (Wt Pct)	38.28	42.1	8.7	1.62	1.82	1.23	1.1	0.18	4.97

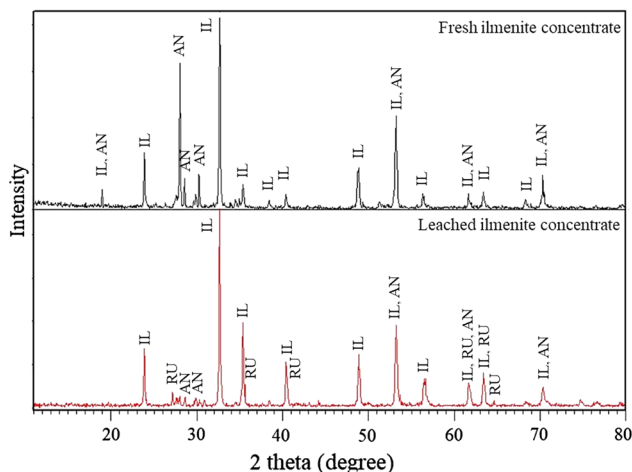


Fig. 7—XRD pattern of the solid residual (optimization test).

ACKNOWLEDGMENT

The authors acknowledge access to infrastructure from the Mining Engineering Department, Isfahan University of Technology.

REFERENCES

- H. Salehi, H. Aghajani, and H. Salimkhani: *Chem. Eng. Trans.*, 2018, vol. 66, pp. 397–402.
- J.A. Ober: *USGS (US Geological Survey)*, USGS, Reston, VA, 2018.
- N. El-Hazek, T.A. Lasheen, R. El-Sheikh, and S.A. Zaki: *Hydrometallurgy*, 2007, vol. 87, pp. 45–50.
- U. Diebold: *Surf. Sci. Rep.*, 2003, vol. 48, pp. 53–229.
- E. Quagliarini, F. Bondioli, G.B. Goffredo, A. Licciulli, and P. Munafò: *J. Cult. Herit.*, 2012, vol. 13, pp. 204–09.
- J. Kasanen, M. Suvanto, and T.T. Pakkanen: *J. Appl. Polym. Sci.*, 2009, vol. 111, pp. 2597–2606.
- M. Nikolova, A. Genov, S. Valkov, E. Yankov, D. Dechev, N. Ivanov, R. Bezdushnyi, and P. Petrov: *J. Phys. Conf. Ser.*, 2018, vol. 992, p. 012032.
- N. Li, G. Liu, C. Zhen, F. Li, L. Zhang, and H.M. Cheng: *Adv. Funct. Mater.*, 2011, vol. 21, pp. 1717–22.
- J. Lademann, H.J. Weigmann, C. Rickmeyer, H. Barthelmes, H. Schaefer, G. Mueller, and W. Sterry: *Skin Pharmacol. Physiol.*, 1999, vol. 12, pp. 247–56.
- C. Wang, Q. Li, and R.D. Wang: *Mater. Lett.*, 2004, vol. 58, pp. 1424–26.
- N.K. Renuka, A.K. Praveen, and K.K. Aravindakshan: *Mater. Lett.*, 2013, vol. 91, pp. 118–20.
- T. Sreethawong, Y. Suzuki, and S. Yoshikawa: *J. Solid State Chem.*, 2005, vol. 178, pp. 329–38.
- T. Sugimoto and X. Zhou: *J. Coll. Interface Sci.*, 2002, vol. 252, pp. 347–53.
- E. Muniz, M. Góes, J. Silva, J.A. Varela, E. Joanni, R. Parra, and P.R. Bueno: *Ceram. Int.*, 2011, vol. 37, pp. 1017–24.
- T. Peng, D. Zhao, K. Dai, W. Shi, and K. Hirao: *Phys. Chem.*, 2005, vol. 109, pp. 4947–52.

- F. Wu, X. Li, Z. Wang, C. Xu, H. He, A. Qi, X. Yin, and H. Guo: *Hydrometallurgy*, 2013, vol. 140, pp. 82–88.
- T. Tao, Q.-Y. Chen, H.-P. Hu, Z.-L. Yin, and Y. Chen: *Trans. Nonferrous Met. Soc. China*, 2012, vol. 22, pp. 1232–38.
- A.R. Gharakhlou and M.N. Sarvi: *Mater. Res. Express*, 2017, vol. 4, p. 025027.
- D. Aphairaj, T. Wirunmongkol, S. Pavasupree, and P. Limsuwan: *Energy Procedia*, 2011, vol. 9, pp. 539–44.
- T.H. Nguyen and M.S. Lee: *Miner. Process. Extract. Metall. Rev.*, 2018, pp. 1–17.
- M.J. Gázquez, J.P. Bolívar, R. García-Tenorio, and F. Vaca: *J. Hazard. Mater.*, 2009, vol. 166, pp. 1429–40.
- X. Wang, C. Li, H. Yue, S. Yuan, C. Liu, S. Tang, and B. Liang: *Chin. J. Chem. Eng.*, 2019, vol. 27, pp. 575–86.
- F. Habashi, F. Kamaledine, and E. Bourricaudy: *Conf. Metall. Proc. COM 2014*, Montreal, PQ, Canada, 2014.
- C. Li, B. Liang, H. Song, J.-Q. Xu, and X.-Q. Wang: *Microporous Mesoporous Mater.*, 2008, vol. 115, pp. 293–300.
- X. Xiong, Z. Wang, F. Wu, X. Li, and H. Guo: *Adv. Powder Technol.*, 2013, vol. 24, pp. 60–67.
- C. Li, B. Liang, L.H. Guo, and Z.B. Wu: *Miner. Eng.*, 2006, vol. 19, pp. 1430–38.
- S. Wahyuningsih, A. Ramelan, E. Pramono, P. Argawan, A. Djatisulistya, F. Firdiyono, E. Sulistiyono, and P. Sari: *IOP Conf. Ser.: Mater. Sci. Eng.*, 2018, vol. 333, p. 012049.
- J.H. Braun, A. Baidins, and R.E. Marganski: *Prog. Organ. Coat.*, 1992, vol. 20, pp. 105–38.
- H. Bordbar, A.A. Yousefi, and H. Abedini: *Polyol. J.*, 2017, vol. 4, pp. 149–73.
- S. Middlemas, Z.Z. Fang, and P. Fan: *Hydrometallurgy*, 2013, vol. 131, pp. 107–13.
- W. Zhang, Z. Zhu, and C.Y. Cheng: *Hydrometallurgy*, 2011, vol. 108, pp. 177–88.
- W.P. Duyvesteyn, B.J. Sabacky, D.E.V. Verhulst, P.G. West-Sells, T.M. Spitler, A. Vince, J.R. Burkholder, and B.J.P.M. Huls: U.S. Patent 6375923B1, Washington, DC.
- G. McNulty: *NORM V Int. Conf.*, Seville, Spain, IAEA, Wien, Austria, pp. 169–89.
- M.J. Gázquez, J.P. Bolívar, R. Garcia-Tenorio, and F. Vaca: *Mater. Sci. Appl.*, 2014, vol. 2014.
- T. Hiraki, Y. Maruyama, Y. Suzuki, S. Itoh, and T. Nagasaka: *Int. J. Miner. Metall. Mater.*, 2018, vol. 25, pp. 729–36.
- C. McKinley and A. Ghahreman: *Miner. Process. Extract. Metall.*, 2018, vol. 127, pp. 157–68.
- B. Liang, C. Li, C. Zhang, and Y. Zhang: *Hydrometallurgy*, 2005, vol. 76, pp. 173–79.
- S.A. Berkovich: U.S. Patent 3903239A.
- M. Imahashi and N. Takamatsu: *Bull. Chem. Soc. Jpn.*, 1976, vol. 49, pp. 1549–53.
- E. Olanipekun: *Hydrometallurgy*, 1999, vol. 53, pp. 1–10.
- L. Wei, H. Hu, Q. Chen, and J. Tan: *Hydrometallurgy*, 2009, vol. 99, pp. 39–44.
- C. Sasikumar, D.S. Rao, S. Srikanth, N.K. Mukhopadhyay, and S.P. Mehrotra: *Hydrometallurgy*, 2007, vol. 88, pp. 154–69.
- R. Vásquez and A. Molina: *Miner. Eng.*, 2012, vol. 39, pp. 99–105.
- N. Jabit and G. Senanayake: *J. Phys. Conf. Ser.*, 2018, vol. 1082, p. 012089.
- F. Wu, X. Li, Z. Wang, L. Wu, H. Guo, X. Xiong, X. Zhang, and X. Wang: *Int. J. Miner. Process.*, 2011, vol. 98, pp. 106–12.
- J.P. van Dyk, N.M. Vegter, and P.C. Pistorius: *Hydrometallurgy*, 2002, vol. 65, pp. 31–36.
- D. Chateigner: *Combined Analysis*, Wiley, New York, 2013, pp. 41–90.
- E. Azimi, S. Karimipour, Z. Xu, J. Szymanski, and R. Gupta: *Int. J. Coal Prep. Util.*, 2017, vol. 37, pp. 12–32.

49. B.N. Akhgar, M. Pazouki, M. Ranjbar, A. Hosseinnia, and R. Salarian: *Chem. Eng. Res. Des.*, 2012, vol. 90, pp. 220–28.
50. N. Aslan: *Powder Technol.*, 2008, vol. 185, pp. 80–86.
51. D.C. Montgomery: *Design and Analysis of Experiments*, Wiley, Hoboken, NJ, 2017, pp. 328–404.
52. E. Azimi, S. Karimipour, M. Rahman, J. Szymanski, and R. Gupta: *Energy Fuels*, 2013, vol. 27, pp. 5595–5606.
53. S. Karimipour, R. Gerspacher, R. Gupta, and R.J. Spiteri: *Fuel*, 2013, vol. 103, pp. 308–20.
54. Z.R. Lasic: *Design of Experiments in Chemical Engineering: A Practical Guide*, Wiley, New York, NY, 2006, pp. 262–367.
55. B. Oraon, G. Majumdar, and B. Ghosh: *Mater. Des.*, 2006, vol. 27, pp. 1035–45.
56. N. Aslan: *Powder Technol.*, 2007, vol. 174, pp. 127–33.
57. Stat-Ease version 7.0.0, Stat-Ease, Inc., Minneapolis, MN.
58. R. Sen: *J. Chem. Technol. Biotechnol. Int. Res. Process. Environ. Clean Technol.*, 1997, vol. 68, pp. 263–70.
59. R.G. Haverkamp, D. Kruger, and R. Rajashekar: *Hydrometallurgy*, 2016, vol. 163, pp. 198–203.
60. C. Li, B. Liang, and H. Wang: *Hydrometallurgy*, 2008, vol. 91, pp. 121–29.
61. T. Lasheen: *Hydrometallurgy*, 2005, vol. 76, pp. 123–29.

Publisher's Note Springer Nature remains neutral with regard to jurisdictional claims in published maps and institutional affiliations.